OPEN ACCESS
IOP Publishing
Smart Materials and Structures
Smart Mater. Struct. **32** (2023) 044004 (10pp)
https://doi.org/10.1088/1361-665X/acc148

# Design and proof-of-concept of an advanced protective system for the dissipation of tangential impact energy in helmets, based on non-Newtonian fluids

**Giuseppe La Fauci**[1], **Mariafederica Parisi**[1], **Alessandro Nanni**[1,4], **Lorenzo Crosetta**[1], **Nicola M Pugno**[2,3] **and Martino Colonna**[1,4,*]

[1] Sport Technology LAB, DICAM, University of Bologna, Via Terracini 28, 40131 Bologna, Italy
[2] Laboratory for Bioinspired, Bionic, Nano, Meta Materials and Mechanics, Department of Civil, Environmental and Mechanical Engineering, University of Trento, Via Mesiano 77, 38123 Trento, Italy
[3] School of Engineering and Materials Science, Queen Mary University of London, Mile End Road, E1 4NS London, United Kingdom
[4] RE-SPORT srl, via Fanin 48, 40127 Bologna, Italy

E-mail: martino.colonna@unibo.it

Received 8 October 2022, revised 24 February 2023
Accepted for publication 3 March 2023
Published 16 March 2023

**Abstract**
We have designed and tested a device based on non-Newtonian fluids for the attenuation of tangential impacts energy in helmets. A shear thickening fluid based on borurated silicones has given the best results in terms of impact energy attenuation in a system that selectively mimics tangential impacts and for this reason it has been used to fill the chamber of a pad, prepared by additive manufacturing, for impact energy dissipation. The pad is composed of a case containing the fluid in which is immersed a rigid pin that is free to move in all direction and therefore is able to absorb energy during its movement inside the fluid. A motorcycle helmet, already composed of two concentrical expanded polystyrene (EPS) liners, has been implemented with seven pads between the two EPS layers. The two layers have only been connected by means of the dissipating pad and are free to rotate and to dissipate energy during the rotation. The results of oblique impacts according to ECE 22.06 with three impact positions, shows a reduction of the brain injury criterion of 14% for the helmet with the pads, compared to the standard helmet, with values well below the threshold imposed by the norm. On the contrary, the maximum of the peak rotational acceleration show a 3% increase. Nevertheless, the rotational acceleration versus time curves indicates that in all three orientations the time of the maximum is shifted towards longer times for the helmets with the pads, indicating that the pads retard the acceleration of the head due to the efficient rotation of the two EPS parts connected by the pads. The described system could be implemented with minimal modifications in existing protective sport and motorcycle helmets.

* Author to whom any correspondence should be addressed.

Supplementary material for this article is available online

Keywords: tangential impacts, helmets, non-Newtonian fluids

(Some figures may appear in colour only in the online journal)

## 1. Introduction

Helmets safety has been significantly improved in the last years thanks to systems able to reduce linear accelerations, caused by impacts [1–3]. Examples of these systems are Wavecel and Koroyd [4] tubular structures and multi-density layered liners [5]. However, it is widely reported in the literature since the 40s of the last century [6] that tangential impacts are the most dangerous ones since they can generate rotational accelerations that are the cause of concussion and traumatic brain injuries [7–9]. For this reason, both helmet producers and standardizing bodies have started to take into consideration oblique impacts and rotational accelerations in order to produce safer helmets. In particular, from the standardizing bodies side, FIM (Fédération Internationale de Motocyclisme—World Motorcycling Association) has been the first that has taken into consideration oblique impacts for motorcycle racing helmets with the standard FRHPhe [10], followed in 2021 by the European Community with the norm ECE 22.06. In these tests, impacts are performed using an oblique anvil. Therefore, during the impact, the linear movement of the falling helmet is partially converted into rotation, which magnitude and duration is monitored trough accelerometers positioned in the headform center of gravity and connected to a data acquisition system.

From the producer point of view, the systems that are nowadays available for the mitigation of rotational acceleration are based on the reciprocal movement of the external and internal part of the helmet. The most used system for impact energy attenuation is MIPS [11] (which acronym means Multi-directional Impact Protection System) that is a system developed and patented by a spin-off company of KTH University in Stockholm in 2007. This system is composed by a thin plastic layer in the internal part of the helmet, connected with elastic bands to the outer part of the helmet [12]. This layer moves, during an oblique impact, along with the head, thus retarding the moment in which the rotational forces reach the head. Scientific literature report that this system can decrease the rotational acceleration by almost 40% [13]. However, a recent paper [14] has shown that when a biofidelic scalp layer is present, there is no statistical difference between helmet models with and without the MIPS in terms of rotational acceleration, velocity, relative rotation, impact duration and injury risk, indicating that the previous studies—which have not tested anti-rotational acceleration technologies in the presence of a realistic scalp layer—may have exaggerated the contribution of such technologies. Moreover, after a certain rotation, the rubber bands, being made of an elastomer, may get to their extension limit and could break or arrive to a point in which are not able to further elongate, thus transferring the impulse to the head. Therefore, those systems may be able to absorb only a low amount of energy during the movement, only retarding the moment in which the impulse is transferred to the head.

An alternative system has been implemented by 6D [15] that has produced a helmet, named ATR 2, with a series of elastomeric pads that connects the inner and outer part of the helmet. However, even if the elastomers are of larger dimensions compared to those of MIPS system, for the same motivation stated above, they may be not able to significantly dissipate the energy of an impact but, again, just to retard the translation of the head relatively to the helmet.

A recent paper [16] has compared helmets with MIPS and 6D systems, indicating that MIPS systems reduce the brain injury criterion (BrIC) and peak rotational accelerations with respect to standard helmets while the 6D systems increases the values. However, in the paper different helmets with 6D and MIPS systems have been compared so it cannot be stated clearly which system is better, since the differences could arise from the other characteristics of the helmets (stiffness of the external part, thickness of expanded polystyrene (EPS), etc). In order to overcome the potential issues connected with the existing systems, we have developed a modular system that not only allows the movement of the external part of the helmet with respect to the head, but also dissipates energy during the movement [17]. The idea at the base of our approach is based on a system in which a moving object is immersed in a fluid that permits the motion of the object (and therefore of the external part of the helmet with respect to the head) but that also dissipate energy during its movement. This is similar to what happens in train-bumpers or in vehicles shock absorbers. Moreover, this system is interposed between the EPS foam layers and not in the inner part of the helmet as for the MIPS system and therefore is not affected by the scalp shape and type.

It is well known that energy dissipation performed by fluids depends on their viscosity and on their overall rheological properties [18]. Non-Newtonian fluids are widely used in impact energy dissipation attenuation due their unique behavior of changing their viscosity at different shear rates [19, 20]. Examples in body protection systems are D3O [21] and PolyAnswer [22] materials. The two main classes of non-Newtonian fluids are shear-thickening (if viscosity increases with the shear rate) and shear-thinning (if viscosity decreases with the shear rate) fluids [23] (figure 1), both used in impact energy damping applications [18]. Most polymeric materials have a shear-thinning behavior in the molten state and in solution [24], while macromolecules with strong intermolecular forces between polymer chains (e.g.

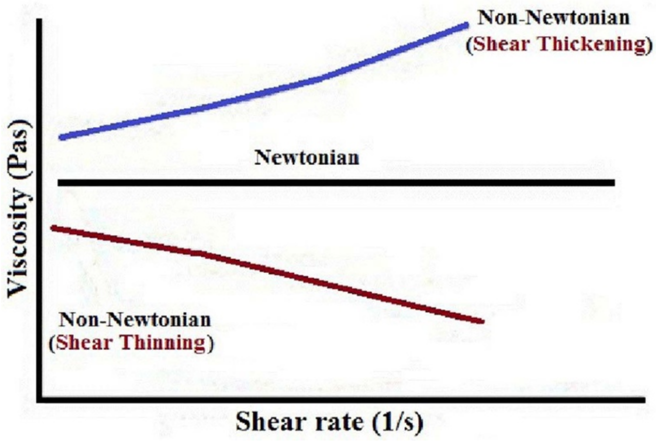


**Figure 1.** Viscosity vs shear rate for Newtonian and non-Newtonian fluids.

starch and borurated silicones) exhibit a shear-thickening behavior [19, 25].

We have previously tested and modeled several back-protectors containing shear-thickening fluids, showing that they behave mainly as soft materials at low shear rates. This behavior allows a good ergonomic comfort when moved at low speed. On the contrary, at high shear rates the material becomes stiffer, thus distributing the impact energy on a wider area and spreading the impact time on wide time-frame, decreasing the transmitted impact force [26–28]. In several cases, the non-Newtonian material used is a borurated silicon (PBDMS) that creates non-permanent and time dependent cross-links between polymer chains (figure 2).

In order to produce body-protectors these fluids are generally incorporated into a foam, generally thermoplastic polyurethane (TPU) or ethylene vinyl acetate (EVA) based, with the aim to keep them confined. Also in helmets, LEATT [29] uses a non-Newtonian foam for the production of turbine-shaped parts that are in connection with the head (LEATT Turbine 360°) [30]. However, in this case the deformation of the foam is caused by the friction of the part with the head of the user and therefore may not be able to provide a significant energy dissipation due to the low friction with hairs and, moreover, it is dependent from the scalp shape and type.

Some producers have also started using non-Newtonian fluids encapsulated in flexible bags. For example, Fox Racing with the Fluid Inside system [31] and POC with the Spin system [32] have created helmets having small bags containing encapsulated fluids that are positioned on the inner liner in direct contact with head. The effect of a shear force may be not able to produce a significant deformation of the bags due to their thin shape and to the low friction that occurs between the head and the bags and for this reason a low energy absorption should be expected. Moreover, this effect should be dependent from the shape and type of scalp [14].

Accordingly, none of the existing systems may be able to both guarantee a mobility between the inner and outer part of the helmet and, at the same time, to dissipate energy in all directions during this movement and, at the same time,

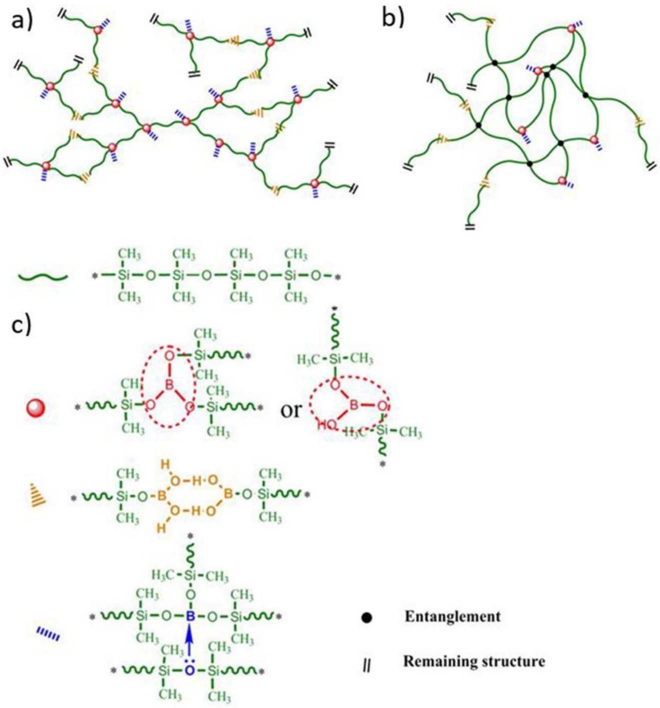


**Figure 2.** Schematic illustration of the physical interactions for polyborosiloxane (PBDMS). (a) PBDMS obtained from precursors with low molecular masses (no topological entanglements). (b) PBDMS obtained from precursors with high molecular masses (topological entanglements). (c) Reversible and irreversible interactions occurring in PBDMS.

being independent from the scalp type and shape [14]. For this reason, we have designed and 3D printed a pad composed of a rigid lower part containing a fluid in which is immersed a rigid pin that is free to move in all directions dissipating energy during its movement (figure 3). The pad is closed in the upper part with a flexible gasket and the upper part of the module is fixed to the external EPS liner of the helmet while the lower part is connected with the internal EPS liner of the helmet. The internal and external liners are only connected by means of the dissipating pads and therefore are free to rotate while absorbing rotational energy (figure 3).

In this paper we report, the proof-of-concept and the application of this novel impact energy attenuation system based on non-Newtonian fluids. In the first part we have prepared and characterized the non-Newtonian fluids. We have then tested in tangential impacts a single pad in order to determine the best fluid to be used and finally we have implemented a commercial motorcycle helmet with the pads and performed impacts according to EN 22.06 on the helmet.

## 2. Methods

### 2.1. Materials

Hydroxy-terminated polydimethylsiloxane (PDMS) precursor with weight-average molecular mass (specified by the supplier) of 4200 g mol$^{-1}$, was purchased from Alfa Aesar Company.

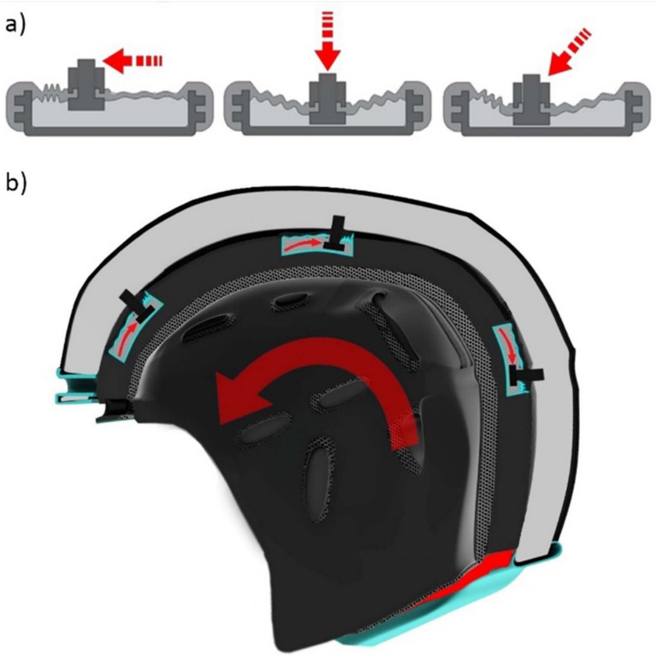


**Figure 3.** (a) Impact energy attenuation modules that can absorb tangential, normal and combined impacts. (b) Section of the design of the helmet with the impact attenuation modules.

Boric acid (BA) (B0394), the silicone used as shear thinning fluid and n-hexane (ReagentPlus® ⩾99%) were all provided by Sigma-Aldrich Company.

A set of commercial Airoh Aviator 2.3 Motocross Helmet was provided by Locatelli S.P.A.

### 2.2. Fluid preparation

PDMS and finely ground BA were previously dried at 50 °C in a vacuum oven overnight prior to use. To prepare the polyborodimethylsiloxane (PBDMS), BA was dispersed in the PDMS precursor with the stoichiometric ratio, $r = 1$ (the mass fraction of the hydroxyl groups of BA to those of PDSM). The mixture was stirred at room temperature for 2 h and then kept at the same temperature for 24 h to allow further reaction.

The obtained raw PBDMS, was purified in n-hexane (previously dried by using molecular sieves) in order to remove all the unreacted BA. The PBDMS solution was vacuum-filtered through a polyvinylidene fluoride membrane and finally, the purified product was collected after evaporation of the solvent at 60 °C and then further dried at 60 °C in a vacuum oven overnight. The occurrence of the boruration reaction was analyzed by Fourier transform infrared (FTIR) spectroscopy using a Perkin Elmer Spectrum One FTIR infrared spectrometer.

### 2.3. Fluid characterization

Rheological tests were carried out on an Anton Paar EC-Twist 502 rheometer, using a plate-plate geometry (25 mm in diameter). The rheometer is equipped with a Peltier control system that provide a precise control of temperature (±0.1 °C).

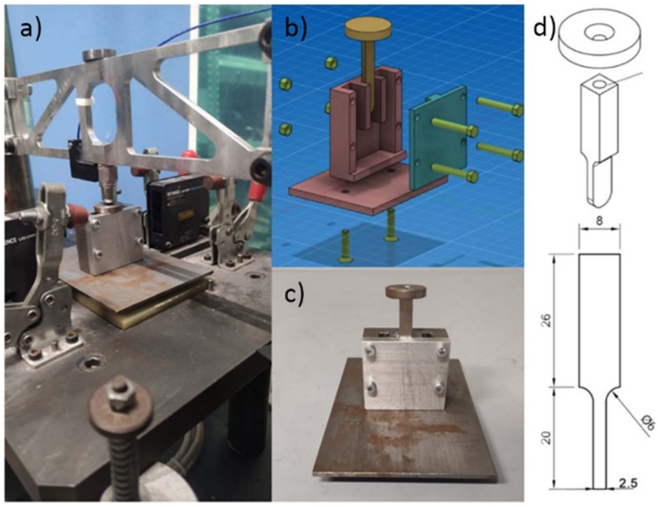


**Figure 4.** (a) Impact set-up for selective tangential impacts during tests. (b) Impact device assembly. (c) Assembled device. (d) Technical drawing of the impact device.

In order to obtain highly accurate results, the zero-gap position was determined using an automatic gap control function. Furthermore, before each rheological test, a steady pre-shear was applied on the sample to remove the possible effects of any previous shear history, allowing the material to reach its equilibrium state.

The frequency-sweep tests were performed at 25 °C with a strain amplitude of 0.1% and a frequency range from 0.001 to 0.1 Hz.

### 2.4. Compression tests at different shear rates

Compression tests were conducted on an INSTRON 5966 series machine. All tests were performed at 23 °C applying different shear rates (10, 50, 100, 150 and 200 mm min$^{-1}$) on the system reported in figure 4 filled with shear-thickening and shear-thinning fluids.

### 2.5. Tangential impact test on a single module

Impact tests were conducted on a system that simulates the pad behavior considering only tangential impacts (figure 4). The custom-made apparatus has been manufactured from aluminum and steel, carved with a computerized numerical control (CNC) machine. The system has a chamber (41 × 21 × 10 mm) filled with PBDMS that can be deformed by a round-tip nail with a cross section of 8 × 2.5 mm and 20 mm length. A flat impactor with 15 mm of diameter was directly connected with a PCB 208C05 load cell (with 22.2 kN upper limit). Data have been acquired through a National Instrument USB 9215 system at 100 kHz. A set of impact tests at 1.25 and 2.50 J have been performed on the system built to mimic the tangential impacts (figure 4). The effective impact energy has been evaluated by measuring the mass of the impactor, the drop height and the impact speed with a laser detection system model MICRO-EPSILON opto ncdt1402-200. The energy impacts have been chosen on the base of the

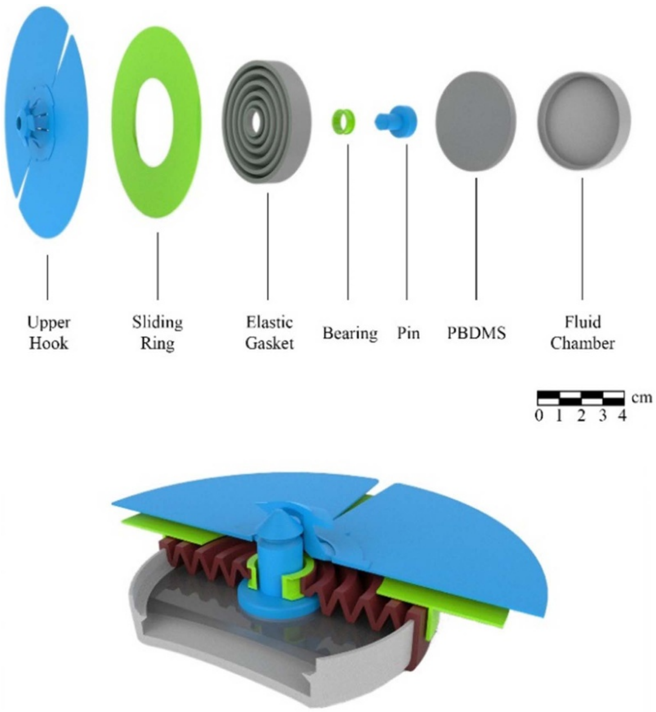


**Figure 5.** Elements of the pad and their position.


**Figure 6.** (a) Front and lateral views of AIROH Aviator 2.3 helmet. (b) EPS liners of the helmets with pads and sliding layer before the final assembly.

assumption that more modules will be present in the complete helmet and most of the impact energy is generally transferred perpendicularly to the surface. The load cell in the impactor has been used to monitor the time/force impact curves for the empty system and for the system with the internal chamber filled with the two non-Newtonian fluids. Three impacts have been performed on all combination of fluids and impact energies, and the results averaged.

### *2.6. Pads manufacturing*

The pads were prepared by additive manufacturing. All the rigid components were printed using a Makerbot Method X FDM printer, using a Formfutura Tough PLA filament in order to achieve both resistance and rigidity, while an Easyfill PLA was used for the parts that needed a low-grip surface for sliding. The low friction layer was made by a 0.15 mm low density polyethylene (LDPE) film. For the elastic gasket, a series of casts was made by additive manufacturing. The material used for the gasket casting was a Prochima Sintagom 703-30 polyurethane with Shore A hardness of 25 (declared by the producer) and a curing period of 24 h at a temperature of 50 °C.

The pads are composed of six parts (figure 5). The base chamber is embedded in the inner liner and filled with PBDMS, the pin with its bearing is positioned in the chamber and the elastic gasket is mounted on the top of it to seal the system. The shape of the base chamber has the same curvature of the EPS liner. The same curvature is present also on the lower face of the moving pin (figure 1 supporting info).

The sliding ring has been screwed on the chamber and gasket to allow a solid interlocking of the components and to offer a low friction sliding surface.

The six parts have been assembled with the sequence reported in figure 5, filled with PBDMS and sealed (figure 2 in supporting info). The total mass of the single pad filled with PBDMS is 12 g.

### *2.7. Helmet assembly*

The system composed of seven pads was embedded in an Airoh Aviator 2.3 production helmet (figure 6). This helmet has been chosen since it already contains an EPS liner made of two concentric parts, that permits a free movement between the parts. A sliding surface made of an LDPE film of 0.15 mm thickness has been interposed, in the modified helmet, between the two EPS parts to decrease the friction due to EPS to EPS contact. A series of seven hooks and the LDPE sliding layer have been screwed in the same position as the pads in the inner liner (figure 6). The two EPS liners were then positioned and the seven pins have been fastened in the corresponding hooks. In this way the system is composed by two liners that can reciprocally move and rotate through the pins. The total mass added to the helmet for the entire system is 84 g and, considering an original weight of 1070 g, the weight increment corresponds to 7.85%.

### *2.8. Impact tests on helmet*

Two helmets were tested according to ECE 22.06 norm for oblique impacts, one in standard configuration (without the rotational dissipation system) and the second with the rotational dissipation system with seven pads containing the shear thickening fluid. The tests were performed using an AD Engineering ECE 22.06 homologated machine and a DLS9000

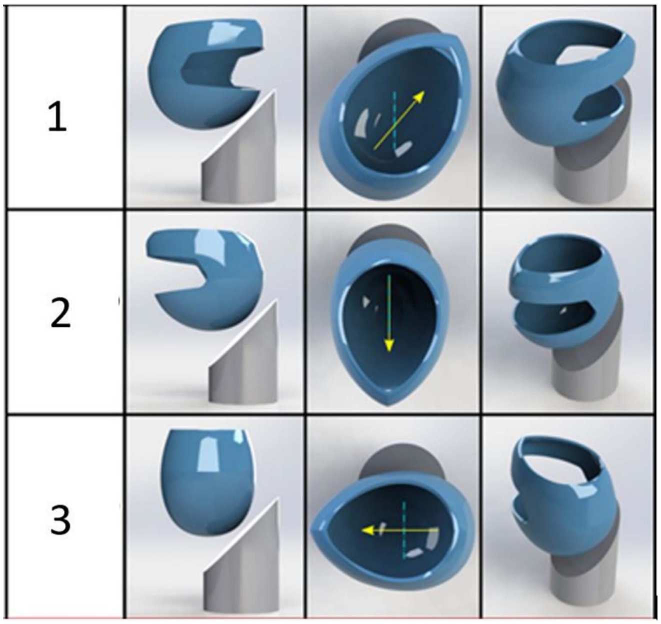


**Figure 7.** Impact positions for ECE 22.06.

data logging system. All the tests were performed in complying with the ECE 22.06 norm. Tests were made with a final impact velocity of 8.20 m $s^{-1}$ and repeated three times on different impact points for every helmet. The headform used as a human head surrogate in the testing of protective helmets is a three dimensional approximation of the human head, excluding facial features and pinnae, which contains a housing for the measuring equipment (accelerometers sensors) in its center of gravity. In compliance with ECE 22.06 homologation norm, the headform used for the tests was made of a metal with characteristics that does not give rise to resonance at frequencies below 3000 Hz. The accelerometers acquisition frequency used in the headform was 10 kHz.

Due to the presence of accelerometers in the headform it was possible to determine rotational accelerations (rad $s^{-2}$) during the impact and to determine the BrIC, as a diffuse axonal injury criterion [33], that was calculated as follow [33, 34]:

$$\mathrm{BrIC} = \sqrt{\left(\frac{\omega_{x-\max}}{\omega_{x\mathrm{C}}}\right)^2 + \left(\frac{\omega_{y-\max}}{\omega_{y\mathrm{C}}}\right)^2 + \left(\frac{\omega_{z-\max}}{\omega_{z\mathrm{C}}}\right)^2}$$

where $\omega_{x-\max}$, $\omega_{y-\max}$ and $\omega_{z-\max}$ are the maximum rotational velocity around *X, Y*, and *Z* axes respectively and $\omega_{x\mathrm{C}}$, $\omega_{y\mathrm{C}}$ and $\omega_{z\mathrm{C}}$ are the critical angular velocities in their respective directions, with values of 66.25, 56.45 and 42.87 rad $s^{-1}$ respectively. The peak of rotational acceleration (PRA) was also monitored as an indication of acute subdural hematoma criterion. The oblique impacts have been performed at three different points. These three impact directions and positions have been chosen since they are acting along the sagittal plane of the helmet (position 2), perpendicular to the sagittal plane (position 3) and at 45° respect to the sagittal plane (position 1) (figure 7).

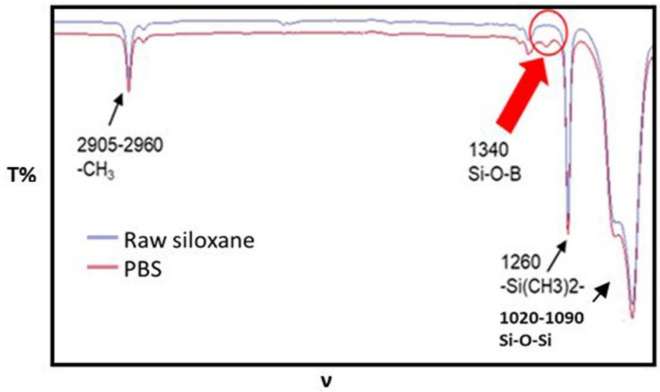


**Figure 8.** FT-IR spectra of PBDMS and siloxane precursor (PDMS).

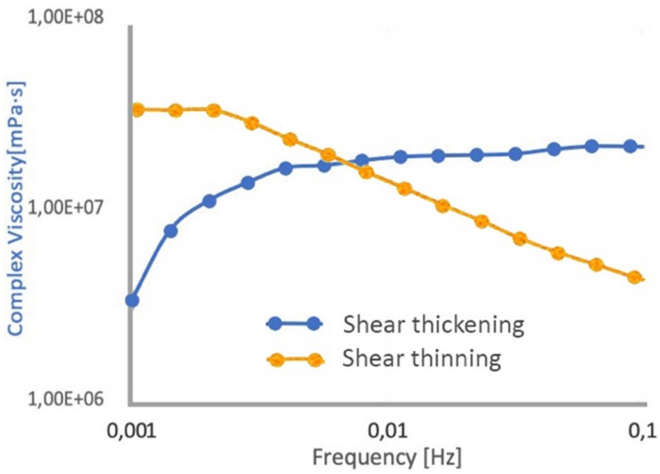


**Figure 9.** Complex viscosity of PBDMS fluid and silicone fluid as a function of frequency.

## 3. Results

### *3.1. Fluid characterization*

The boruration was confirmed, according to the literature [25, 35] by Fourier transform infrared spectroscopy detecting the presence of cooperative bonding between boron and oxygen. The spectra of the resulting PBDMS showed the presence of the characteristic absorption bands indicating the presence of $Si(CH_3)_2$ and Si–O groups at 1260 $cm^{-1}$ and 1020–1090 $cm^{-1}$. The formation of Si–O–B bonds has been confirmed by the peak at 1340 $cm^{-1}$ as a result of the successful condensation between OH– groups from both siloxane and BA (figure 8).

The complex viscosity analysis shows that both non-Newtonian fluids have a strong frequency dependent behavior (figure 9). In particular, an increase of the viscosity by increasing the frequency (thus showing a shear thickening behavior) was observed for PBDMS while silicone shows a decrease of the complex viscosity, with a clear shear thinning behavior.

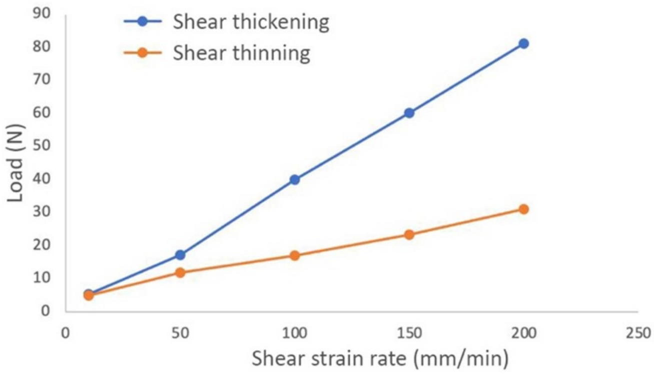


**Figure 10.** Load at 10 mm displacement as a function of shear strain rate.

### *3.2. Tests at different shear rates*

An increase of the load/displacement curves with shear strain rate has been observed for the system filled with both fluids (figures 3 and 4 in supporting info). However, if we compare the load at 10 mm strain (that for both systems is in the plateau region of the stress/strain curve), as a function of shear strain rate (figure 10) it is possible to observe how the shear thickening material is more affected by shear rate with respect to the shear thinning one.

### *3.3. Tangential impact tests*

The impact tests results shows (figure 11), at both impact energies, that the presence of the fluids decreases the maximum peak force and increases the time-to-peak compared to the empty system. These two features are the most important to spread the impact on a wider time frame and with a lower maximum force, clearly indicating that the presence of the fluid is able to dissipate the tangential impact energy. In particular, the use of PBDMS reduced the maximum of the transmitted impact force of 80 ± 3% at 1.25 and of 55 ± 5% at 2.5 J compared to fluid absence and the time to peak was postponed of over 10 ms. The use of a non-borurated silicone, with a shear thinning behavior, only reduces the impact force of 40 ± 5% at 1.25 J and of 30 ± 5% 2.5 J compared to the rigid system even if it has a higher viscosity at low shear rates compared to PBDMS (see figure 9). Therefore, it is clear how the shear thickening fluid is more efficient in energy dissipation with regards to the shear thinning, especially at the lower impact energy, thus indicating that shear thickening fluids must be preferred over shear thinning fluids for impact energy dissipation even if they have a lower viscosity at low shear rates. An analysis of the impact curves obtained with the shear thickening fluid at 2.50 J impact energy shows how this fluid is at the beginning able to dissipate part of the energy but, after 7 ms from the impact, the moving object touches the end of the box and therefore the peak of the force increases sharply. However, the first part of the impact is able to absorb part of the energy

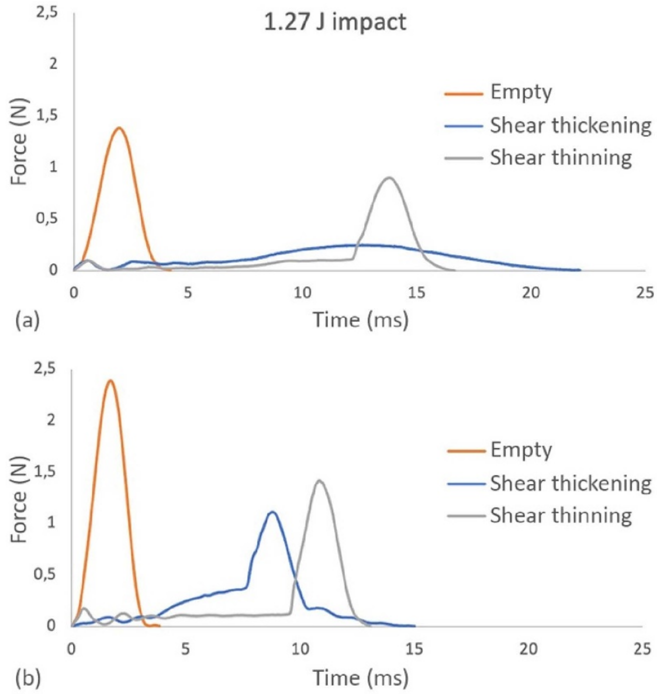


**Figure 11.** Transmitted force measured for the experimental set-up that selectively mimics the tangential impacts at 1.25 J (a) and 2.50 J (b).

and therefore the maximum of the peak is lower compared to the other cases.

### *3.4. Helmet testing*

The results in table 1 show that both helmets have values well below the threshold upper limits reported in ECE 22.06 norm, that are 10 400 rad $s^{-2}$ for rotational accelerations, 0.78 for BrIC and 275 g for translational accelerations. A recent paper [16] that has compared helmets with MIPS and 6D systems has shown values between 0.4 and 0.9 for BrIC and therefore the helmet we have chosen to be implemented with the pads, already has a maximum BrIC value of 0.28 (in position 2) that is well below those of the helmets reported in the cited paper, indicating that the helmet chosen has already high performances.

The rotational acceleration versus time curves (reported in figure 5 in supporting info) indicates that in all three orientations the time of the maximum is shifted towards longer times for the helmets with the pads.

The comparison of the BrIC values reported in table 1 shows that the mean of the values for the helmet with the pads is 14% lower compared to the standard one. On the contrary, a slight increase in the rotational and linear accelerations have been observed for the modified helmet with respect to the standard helmet. In particular, PRA mean values were slightly higher (3%) for the helmet with the pads, mainly due to the higher value in position 3 that corresponds to an impact

**Table 1.** Impact results.

| Helmet | Impact parameter | ECE 22.06 limit | 1 (45°) | 2 (180°) | 3 (270°) | Mean value |
|---|---|---|---|---|---|---|
| No pads | PTA (g) | 275 | 152 | 97 | 160 | 136 |
| | PRA (rad $s^{-2}$) | 10 400 | 3020 | 1692 | 2266 | 2326 |
| | BrIC | 0.78 | 0.25 | 0.28 | 0.17 | 0.233 |
| | Time of max rotational peak (ms) | — | 8 | 8 | 10.5 | 8.83 |
| With pads | PTA (g) | 275 | 168 | 126 | 163 | 152 |
| | PRA (rad $s^{-2}$) | 10 400 | 2529 | 1815 | 2883 | 2409 |
| | BrIC | 0.78 | 0.21 | 0.18 | 0.21 | 0.200 |
| | Time of max rotational peak (ms) | — | 9 | 8.5 | 11.7 | 9.73 |

that is perpendicular to the sagittal plane of the helmet. On the contrary, the values of linear accelerations (peak translational acceleration (PTA)) are slightly higher for the modified helmet in all impact directions tested.

## 4. Discussion

We have prepared and tested non-Newtonian fluids in order to determine the best fluid to be used in the tangential impact attenuation systems, finding that PBDMS is the most appropriate fluid to be used. Impact tests performed on a system that mimics only tangential impacts have shown that the pad we have designed is able work when filled with PBDMS at energies between 1.25 and 2.50 J. However, a different shape of the moving part, a different shape and volume of the chamber and a different type and amount of fluid (for example a PBDMS with a different boron content and therefore different viscosity and shear thickening behavior) should provide different threshold energy values at which the pad is able to efficiently absorb the tangential impact energy. An optimization of these parameters will be performed in future works.

The impact energy attenuation module is composed of a rigid lower part containing a fluid in which is immersed a rigid pin that is free to move in all directions. In this way, the internal and external parts of the helmet are only connected by means of the dissipating pads and are free to rotate and to dissipate energy during the rotation. A system composed of seven pads have been then inserted in a motorcycle helmet already composed of two concentrical EPS liners. The results of oblique impacts according to ECE 22.06 show a mean value reduction of the BrIC of 14% for the helmet with the pads compared to the standard helmet, with values well below the threshold imposed by the norm. This result is even more considerable in consideration of the low BrIC starting values of the standard helmet. The rotational acceleration versus time curves indicates that in all three orientations the time of the maximum is shifted towards longer times for the helmets with the pads, indicating that the pads retard the acceleration of the head due to the efficient rotation of the two EPS parts connected by the pads.

The comparison of the PTA shows small differences between the two helmets with a small increase for the modified helmet in all impact positions, indicating that the pads slightly transfer the translational accelerations to the head. However, this aspect could be improved by increasing the surface area of the moving pin and the viscosity of the fluid in order to absorb more energy during the translational (perpendicular to the surface) movement of the helmet with respect to the head.

The analysis of the peak rotational accelerations shows a slightly higher mean value for the modified helmet. A more detailed look shows that the worst results in terms of PRA of the helmet with the pads are observed for the impact in position 3 that is the one in which the impact occurs perpendicularly to the sagittal plane of the helmet. This type of impact causes a rotation along the axis that is perpendicular to the sagittal plane. A rotation along this axis is more difficult due to the shape of the EPS liner that is not spherical along the axis (see figure 6) especially in the lower part that has almost parallel sides. On the contrary, the shape on the sagittal plane is more spherical and therefore the rotation is less hindered and the pads are able to operate correctly. A more spherical design of the EPS liners could solve this problem. However, due to the limited number of helmets tested it is not possible to draw robust statistical conclusions. More helmets will be prepared and the system will be optimized in future works. An optimization of the number, positioning and dimension of the pads could also permit to have a more constant (and lower) BrIC and PRA for the different types of impacts. This will be implemented in a further optimization process, along with the optimization of the dimension of the moving pins and of the viscosity of the fluids.

Another main limitation of the present work, that must be addressed in the future, is the effect of temperature on the viscosity and on the impact energy dissipation of the fluids. Indeed, viscosity is a temperature-dependent property and most sports that requires the use of helmets are performed in outdoor environment with variable temperatures.

## 5. Conclusions

We have demonstrated on a model system that shear thickening fluids can be used to absorb the energy of tangential impacts and therefore we have implemented a helmet with seven pads containing this type of fluid. The impact tests on two helmets have shown promising results in terms of BrIC reduction and time-to-peak increase for the helmet implemented with the modules containing the fluid.

Further work is therefore in progress, and will be reported in following papers, in order to optimize the dimensions, design and number of modules, shape of the EPS layers and type of shear thickening fluid with the aim to improve also PRA and PTA in all directions of impact, further reduce BrIC and to assess the effect of temperature on the system. The optimization work will be also performed with the aid of Finite Element Model analysis.

## Data availability statement

All data that support the findings of this study are included within the article (and any supplementary files).

## Acknowledgments

The authors thank Locatelli S.p.a. for providing the helmets and for the impact tests on the helmets.

## Conflict of interest

The authors declare that they are developing the system for its potential commercialization in helmets and that some of the authors own the IP rights on the patent that describes the device.

## ORCID iDs

Giuseppe La Fauci https://orcid.org/0000-0001-9211-9954
Mariafederica Parisi https://orcid.org/0000-0001-9361-2222
Alessandro Nanni https://orcid.org/0000-0003-4768-7236
Nicola M Pugno https://orcid.org/0000-0003-2136-2396
Martino Colonna https://orcid.org/0000-0002-5728-6332

## References

[1] Leng B, Ruan D and Tse K M 2022 Recent bicycle helmet designs and direction for future research: a comprehensive review from material and structural mechanics aspects *Int. J. Impact Eng.* **168** 104317

[2] Fernandes F A O and Alves de Sousa R J 2013 Motorcycle helmets—a state of the art review *Accid. Anal. Prev.* **56** 1–21

[3] Bottlang M, Rouhier A, Tsai S, Gregoire J and Madey S M 2020 Impact performance comparison of advanced bicycle helmets with dedicated rotation-damping systems *Ann. Biomed. Eng.* **48** 68–78

[4] Chilson J A, Lloyd J, Rogers J and Storey P Body protecting device *US Patent US10736373-B2*

[5] Bliven E, Rouhier A, Tsai S, Willinger R, Bourdet N, Deck C, Madey S M and Bottlang M 2019 Evaluation of a novel bicycle helmet concept in oblique impact testing *Accid. Anal. Prev.* **124** 58–65

[6] Holbourn A H S 1943 Mechanics of head injuries *Lancet* **242** 438–41

[7] Milne G, Deck C, Carreira R P, Allinne Q and Willinger R 2012 Development and validation of a bicycle helmet: assessment of head injury risk under standard impact conditions *Comput. Methods Biomech. Biomed. Eng.* **15** 309–10

[8] Bourdet N, Deck C, Tinard V and Willinger R 2011 Behaviour of helmets during head impact in real accident cases of motorcyclists *Int. J. Crashworthiness* **17** 51–61

[9] Sahoo D, Deck C and Willinger R 2016 Brain injury tolerance limit based on computation of axonal strain *Accid. Anal. Prev.* **92** 53–70

[10] Fédération Internationale de Motocyclisme 2021 Fédération internationale de motocyclisme June (available at: www.frhp.org/user/pages/documents/FRHPhe-01%20-%20Homologation%20Manual.pdf)

[11] Halldin P 2013 Helmet *U.S. Patent US8578520*

[12] DiGiacomo G, Tsai S and Bottlang M 2021 Impact performance comparison of advanced snow sport helmets with dedicated rotation-damping systems *Ann. Biomed. Eng.* **49** 2805–13

[13] Bonin S J, DeMarco A L and Siegmund G P 2022 The effect of MIPS, headform condition, and impact orientation on headform kinematics across a range of impact speeds during oblique bicycle helmet impacts *Ann. Biomed. Eng.* **50** 860–70

[14] Zouzias D, De Bruyne G, Ni Annaidh A, Trotta A and Ivens J 2021 The effect of the scalp on the effectiveness of bicycle helmets anti-rotational acceleration technologies *Traffic Inj. Prev.* **22** 51–56

[15] 6D Helmets 6D Helmets (available at: www.6dhelmets.com/atr-2/)

[16] Yu X, Logan I, De Pedro Sarasola I, Dasaratha A and Ghajari M 2022 The protective performance of modern motorcycle helmets under oblique impacts *Ann. Biomed. Eng.* **50** 1674–88

[17] Colonna M, Parisi M F and La Fauci G 2021 *Italian Patent* n.102021000021623

[18] Parisi M F, Colonna M and Pugno N M 2023 Use of shear thickening fluids in sport protection applications, a review submitted

[19] Zhao C, Gong X, Wang S, Jiang W and Xuan S 2020 Shear stiffening gels for intelligent anti-impact applications *Cell Rep. Phys. Sci.* **1** 100266

[20] Wang Z G, Yu Z W, Sun Y Y and Li Q Y 2013 Characterization and application of shear thickening fluids *Applied Mechanics and Materials* vol 405–408 (Bäch: Trans Tech Publications, Ltd) pp 2503–6

[21] Ferguson J R 2007 Impact shock absorbing material *U.S. Patent No. US8087101B2*

[22] Mendes Oliveira N D, Couto Oliveira B A and Vieira Ribeiro I A 2016 Absorbent polymeric material, method for producing same and uses thereof *Patent WO2017068513A1*

[23] Pop I and Ingham D 2001 Free and mixed convection boundary-layer flow of non-Newtonian fluids (https://doi.org/10.1016/B978-008043878-8/50013-4)

[24] Ding J, Tracey P, Li W, Peng G, Whitten P G and Wallace G G 2013 Review on shear thickening fluids and applications *Text. Light Ind. Sci. Technol.* **2** 161–73

[25] Tang M, Wang W, Xu D and Wang Z 2016 Synthesis of structure-controlled polyborosiloxanes and investigation on their viscoelastic response to molecular mass of polydimethylsiloxane triggered by both chemical and physical interactions *Ind. Eng. Chem. Res.* **55** 12582–9

[26] Signetti S, Nicotra M, Colonna M and Pugno N M 2019 Modeling and simulation of the impact behavior of soft

polymeric-foam-based back protectors for winter sports *J. Sci. Med. Sport* **22** S65–S70
[27] Dotti F, Ferri A, Moncalero M and Colonna M 2016 Thermo-physiological comfort of soft-shell back protectors under controlled environmental conditions *Appl. Ergon.* **56** 144–52
[28] Nicotra M, Moncalero M, Messori M, Fabbri E, Fiorini M and Colonna M 2014 Thermo-mechanical and impact properties of polymeric foams used for snow sports protective equipment *Proc. Eng.* **72** 678–83
[29] Leatt C J, Keevy P A, Steffens J P and Corp L 2017 *U.S. Patent No. US20170172242A1*
[30] Siegkas P, Sharp D J and Ghajari M 2019 The traumatic brain injury mitigation effects of a new viscoelastic add-on liner *Sci. Rep.* **9** 3471
[31] Fluid Inside (available at: www.fluidinside.com)
[32] POC *POC SPIN Website* (available at: www.pocsports.com/blogs/press-release/poc-presents-spin-and-clarity-brand-new-innovations)
[33] Takhounts E G, Craig M J, Moorhouse K, McFadden J and Hasija V 2013 Development of brain Injury criteria (BrIC) *Stapp Car Crash J.* **57** 243–66
[34] Takhounts E G, Hasija V, Ridella S A, Rowson S and Duma S M 2011 Kinematic rotational brain injury criterion (BRIC) *The 22nd ESV Conf. Proc. (Washington, DC)* vol 11–0263 (available at: www.semanticscholar.org/paper/Kinematic-Rotational-Brain-Injury-Criterion-(BRIC)-Takhounts-Hasija/0691a97a56a2197f2d3fbaf5f5cb4ba786349e03)
[35] Liu Z, Picken S J and Besseling N A 2014 Polyborosiloxanes (PBSs), synthetic kinetics, and characterization *Macromolecules* **47** 4531–7